CHEMISTRY
A EUROPEAN JOURNAL

DOI: 10.1002/chem.200700393

The Role of Fluorine in the Stereoselective Tandem Aza-Michael Addition to Acrylamide Acceptors: An Experimental and Theoretical Mechanistic Study

Santos Fustero,*[a] Gema Chiva,[a] Julio Piera,[a] Alessandro Volonterio,[b] Matteo Zanda,[c] Javier González,[d] and Antonio Morán Ramallal*[d]

Abstract: Aza-Michael additions of α-amino esters to fluorinated acceptors take place in a highly stereoselective manner, to give partially modified Ψ-[$NHCH_2$]retropeptides incorporating a hydrolytically stable trifluoroalanine mimic. The reaction mechanism has been investigated experimentally and theoretically, in order to explain the effect of the trifluoromethyl group on the reactivity and the origins of the experimentally observed stereocontrol. The reaction is a two-step process, involving a tandem aza-Michael addition followed by a stereoselective hydrogen transfer. Both steps are base-catalyzed. The high level of stereocontrol is the result of a combination of electrostatic interactions and steric effects.

Keywords: density functional calculations · diastereoselectivity · fluorine chemistry · Michael reaction · peptides

Introduction

β-Amino carbonyl functionalities are found in a large number of alkaloids and polyketides.[1] Among them, β-amino acids are of crucial importance, as they constitute the structural units of β-peptides, compounds that have proved to be promising biostable peptidomimetics,[2] and so the importance of this field has grown exponentially. In addition, these moieties are versatile building blocks for the synthesis of nitrogen-containing compounds such as 1,3-amino alcohols, β-amino ketones, β-amino acids, and β-lactams.[3]

The most conventional approaches to accessing these derivatives are the Mannich reaction and the conjugate addition of amines and their synthetic equivalents to α,β-unsaturated carbonyls. While the classic Mannich-type protocols often suffer from harsh conditions and long reaction times,[4] the asymmetric aza-Michael reaction has emerged during the last five years as a very powerful tool for the creation of carbon-nitrogen bonds, owing to its simplicity and atom economy. Furthermore, this reaction is economical and environmentally friendly, as no catalyst is generally required in the process. There are three major strategies to achieving asymmetric induction: either by using chiral amines or chiral Michael acceptors or by incorporating chiral ligands in a stoichiometric or catalytic manner.[5] However, the catalytic enantioselective aza-Michael reaction still poses a big challenge in synthetic organic chemistry. Although several efforts have recently been made in this area,[6] to date a general method to perform this transformation is practically unknown.[7]

On the other hand, α-(trifluoromethyl)acrylic acid[8] represents an attractive fluorinated building block for the preparation of fluorinated β-amino acid derivatives[9] and several other classes of biologically active compounds. In this context, in 1991 Ojima described the preparation of fluorinated captopril analogues by conjugate addition of thiolacetic acid to the Michael acceptor derived from α-(trifluoromethyl)-

[a] Prof. Dr. S. Fustero, Dr. G. Chiva, Dr. J. Piera
Departamento de Química Orgánica
Universidad de Valencia
46100 Burjassot, Valencia
and
Laboratorio de Moléculas Orgánicas
Centro de Investigación Príncipe Felipe
46013 Valencia (Spain)
Fax: (+34) 963-544-939
E-mail: santos.fustero@uv.es

[b] Dr. A. Volonterio
Dipartimento de Chimica, Materiali, ed Ingegnieria Chimica
"Giulio Natta Politecnico di Milano via Mancinelli 7
20131 Milano (Italy)

[c] Dr. M. Zanda
C.N.R.-Istituto di Chimica del Riconoscimento Molecolare (ICRM)
via Mancinelli 7, 20131 Milano (Italy)

[d] Prof. J. González, A. M. Ramallal
Departamento de Química Orgánica e Inorgánica
Universidad de Oviedo, 33071 Oviedo (Spain)
E-mail: figf@unioui.es

Supporting information for this article is available on the WWW under http://www.chemeurj.org/ or from the author.

WILEY InterScience DISCOVER SOMETHING GREAT
© 2007 Wiley-VCH Verlag GmbH & Co. KGaA, Weinheim

acrylic acid and L-proline.[10] More recently, Pellacani et al.[11a] have reported a diastereoselective aza-Michael addition of carbamate derivatives to 2-(trifluoromethyl)acrylates, affording different addition products depending on the reaction conditions. Avenoza and co-workers also published a two-step non-Michael-type strategy for the preparation of (*S*)-α-CF_3-isoserine, combining a Sharpless dihydroxylation with the formation of cyclic sulfamidates or sulfates.[11b]

Finally, the highly diastereoselective aza-Michael addition of α-amino esters to *N*-trifluorometacryloyl α-amino acids has recently been reported to be an extremely valuable route to partially modified Ψ[$NHCH_2$]retropeptides incorporating a hydrolytically stable trifluoroalanine mimic.[12,13] The reaction features an unusually high 1,4-asymmetric induction, which is strongly dependent on several experimental factors, such as solvent, catalytic base, R^1 and R^2 chains, and relative stereochemistry of the reaction partners (Scheme 1).

The process might be viewed as a tandem aza-Michael/hydrogen transfer in two steps: a nonstereogenic aza-Michael addition of **1** to **2**, which affords an amide enol intermediate, followed by its tautomerization to **3**, which is the actual stereogenic step.

The highest 1,4-asymmetric induction (up to 42:1) was observed with apolar solvents (such as CCl_4), together with the use of 1,4-diazabicyclo[2.2.2]octane (DABCO) or trimethylamine as catalytic bases[14] and bulky R^1 and R^2 side-chains (such as isopropyl and isobutyl groupings). The hydrogen atom of the newly created stereocenter in the major diastereoisomer of **3** is in an *anti* configuration with respect to the R^2 group (Scheme 1). However, some key aspects, such as the full scope of the reaction and particularly the detailed mechanism of the process and the origin of the diastereoselectivity have remained unsolved until now.

Here we address these two aspects of the process, both from an experimental and from a theoretical point of view.

Abstract in Spanish: *Las adiciones aza-Michael de α-amino ésteres a aceptores fluorados tienen lugar de un modo altamente estereoselectivo, para dar lugar a Ψ-[$NHCH_2$]retropéptidos parcialmente modificados que incorporan un mimético de trifluoroalanina, estable frente a la hidrólisis. El mecanismo de la reacción ha sido investigado experimental y teóricamente, a fin de explicar el efecto del grupo trifluorometilo en la reactividad y en los orígenes de estereocontrol observado experimentalmente. La reacción es un proceso en dos pasos, que implican una adición aza-Michael seguida de una transferencia estereoselectiva de hidrógeno. Ambos pasos están catalizados por una base. El origen del alto grado de estereocontrol radica en una combinación de interacciones electrostáticas y efectos estéricos.*

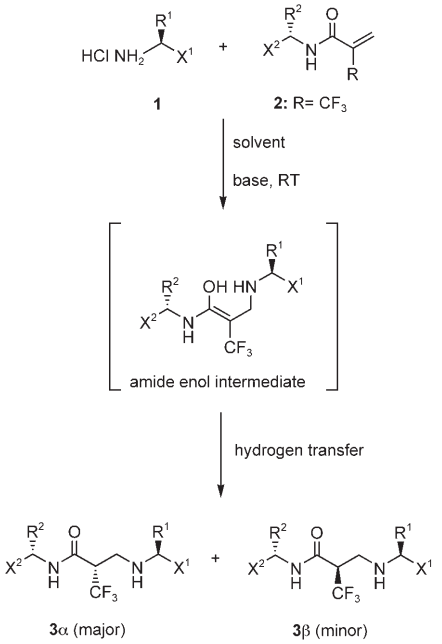

Scheme 1. Stereoselective aza-Michael additions to CF_3-containing acrylamide acceptors.

Results and Discussion

With regard to the scope of the process, several representative examples of nucleophiles **1** and Michael acceptors **2** derived from α-amino ester hydrochlorides and aliphatic amines [such as (*S*)-α-methylbenzylamine and (*S*)-α-methyl-α-naphthylamine] were tested. Table 1 summarizes the results obtained. We observed that, although the process works well independently of the nature of the starting materials, the best results in terms of diastereoselectivity were obtained with Michael acceptors and nucleophiles derived from α-amino esters (entries 1–4, Table 1). An absence of carbonyl groupings in both **1** and **2** considerably reduced the efficiency of the process (entry 12, Table 1), while intermediate situations appear in the cases in which only one carbonyl grouping is present either in the nucleophile (entries 6 and 8, Table 1) or in the Michael acceptor (entries 9–11, Table 1).

With regard to the nature of the R^1 and R^2 chains, we found that the best stereocontrol was achieved with bulky groups such as isobutyl and isopropyl (that is, with leucine and valine derivatives: i.e., *i*Bu > *i*Pr > > Me; see, for example, entries 1 vs 2 and 3 vs 13, Table 1). In addition, no significant effects involving the nature of the ester groupings were observed (entries 2, 3, and 4, Table 1).

Another important aspect of the process, relating to the finally obtained stereoselectivity, is the stereochemistry of the starting partners **1** and **2** (that is, the knowledge of the matched/mismatched pair). The configurations of **1** and **2** thus had a significant effect, as demonstrated by the use of matched/mismatched pairs of the nucleophiles L- and D-Ala methyl esters and the Michael acceptor L-Ala methyl ester

 © 2007 Wiley-VCH Verlag GmbH & Co. KGaA, Weinheim

Table 1. Reactants and conditions in the aza-Michael addition.

Entry[a]	**3**[b]	X^1	R^1	X^2	R^2	dr[c]	Yield [%]
1	**3a**	CO_2Bn	*i*Bu	CO_2Bn	*i*Bu	42:1	95
2	**3b**[d]	CO_2Bn	*i*Pr	CO_2Bn	*i*Pr	38:1	95
3	**3c**	CO_2Me	*i*Pr	CO_2Me	*i*Pr	33:1	89
4	**3d**[d]	CO_2tBu	*i*Pr	CO_2tBu	*i*Pr	33:1	90
5	**3d**	CO_2tBu	*i*Pr	CO_2tBu	*i*Pr	6:1[e]	82
6	**3e**	CO_2tBu	*i*Pr	Ph	Me	17:1[f]	77
7	**3f**	CO_2tBu	*i*Pr	Ph	Me	2:1[g]	78
8	**3g**	CO_2tBu	*i*Pr	α-$C_{10}H_7$	Me	15:1	84
9	**3h**	α-$C_{10}H_7$	Me	CO_2tBu	*i*Pr	6:1	84
10	**3i**	Ph	Me	CO_2tBu	*i*Pr	8:1	64
11	**3j**	Ph	H	CO_2tBu	*i*Pr	8:1	95
12	**3k**	Ph	Me	Ph	Me	3:1	60
13	**3l**	CO_2Me	Me	CO_2Me	Me	9:1[f]	95
14	**3m**	CO_2Me	Me	CO_2Me	Me	2:1[g]	70

[a] The *S*,*S* combination was used unless otherwise indicated. [b] Reaction conditions: DABCO (1 or 2 equiv) (see Experimental Section), CCl_4, 0 °C to RT. [c] Diastereoisomeric ratio (dr) α/β determined by ^{19}F NMR spectroscopy. [d] See ref. [12]. [e] Uncatalyzed reaction. [f] Matched pair: (*S*,*S*,*S*/*S*,*R*,*S*). [g] Mismatched pair: (*R*,*S*,*S*/*R*,*R*,*S*). The *R*,*S* combination (nucleophile **1**, Michael acceptor **2**) was used in this case.

(entries 13 and 14, Table 1), and also with the mixed pair of L-Val *tert*-butyl ester and (*S*)- and (*R*)-α-methylbenzylamine as Michael acceptors (entries 6 and 7, Table 1). In both cases, the *like* **1**/**2** combination (*S*/*S* or *R*/*R*) provided the higher diastereoselectivity; see, for example, **3e** vs **3f** (entries 6 and 7, Table 1), and **3l** vs **3m** (entries 13 and 14, Table 1).

In addition, a comparison of the base-catalyzed vs the uncatalyzed reaction was also studied. Thus, while the diastereoisomeric ratio was 33 to 1 in the case of **3d**, it was only 6 to 1 in the uncatalyzed process (entry 4 vs entry 5, Table 1).

Another interesting feature of this process involves comparison of the reactivities of the fluorinated counterparts on the one hand, and the nonfluorinated ones on the other. For this purpose, acryloyl and metacryloyl Michael acceptors **2** derived from L-valine α-amino *tert*-butyl ester (R = H, Me) were treated with different nucleophiles [such as **1** (X^1 = CO_2tBu, R^1 = *i*Pr and X^1 = Ph, R^1 = H)] (Scheme 2). In all

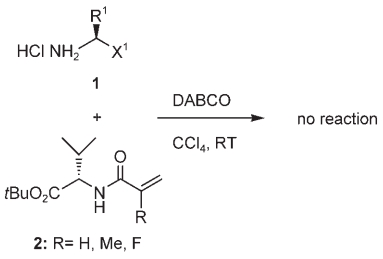

Scheme 2. Unsuccessful aza-Michael additions.

cases, however, under the same reaction conditions (DABCO, CCl_4, and rt), the process did not work at all and the starting materials were recovered. Similar results were obtained when α-fluoroacryloyl Michael acceptors derivatives **2** (R = F) were used as starting materials (Scheme 2).

In the light of these results, we can conclude that the presence of at least one CO grouping in **1** and/or **2** (entries 4, 6, and 10 vs 12), as well as a base (DABCO or Me_3N) as catalyst (entries 4 vs 5), are necessary in order to obtain high 1,4-asymmetric induction. Furthermore, the trifluoromethyl (Tfm) group plays a critical role in the process.

In order to test these mechanistic hypotheses, a theoretical study was carried out. The potential energy surfaces corresponding to the model reactions of acrylamide acceptors **4a–d** (Figure 1) with methylamine and trimethylamine as nucleophile and base, respectively, were explored with the aid of electron density functional theory, with use of the B3LYP/6-31G* hybrid functional.[15]

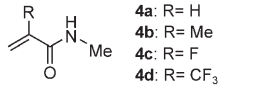

Figure 1. Acrylamide acceptors used in the model calculations.

The theoretical study of the stereochemical course of the reaction was carried out with the Michael acceptors (*S*)-**2l** (R^2 = Me, X^2 = CO_2Me, R = CF_3) and (*S*)-**2c** (R^2 = *i*Pr, X^2 = CO_2Me, R = CF_3), together with the amines (*S*)-**1l**, (*R*)-**1l** (R^1 = Me, X^1 = CO_2Me), and (*S*)-**1c** (R^1 = *i*Pr, X^1 = CO_2Me) (see Scheme 1 and Table 1).

Nucleophilic addition step of methylamine to the Michael acceptors 4a–d: As the starting point of our study, we analyzed the model systems **4a–d**, finding two possible reaction pathways for the nucleophilic addition of the methylamine to the Michael acceptors. The first step of the reaction is the attack of the nucleophilic nitrogen of methylamine at the β-carbon of the α,β-unsaturated system. In the four cases analyzed, the addition reaction appears to start through the formation of a ternary complex **5** between the nucleophile, the Michael acceptor, and the base (trimethylamine) (Figure 2).

Of course, the calculations reported in this work represent the situation under gas-phase conditions, but the experimental situation, which involves the use of nonpolar solvents, such as CCl_4, could be quite similar. In nonpolar solvents such as CCl_4 the formation of these type of hydrogen-bonded complexes can be expected. In all cases, the nucleophilic amine forms a hydrogen bond with the oxygen of the Michael acceptor and the base (that is, the trimethylamine). The geometries of the four complexes **5a–d** are very similar. These complexes are stabilized with respect to the isolated reactants by approximately 4–16 kcal mol^{-1} (Table 2).

The next step in the reaction pathway is the nucleophilic addition of the methylamine to the acrylamide acceptors **4**,

 © 2007 Wiley-VCH Verlag GmbH & Co. KGaA, Weinheim

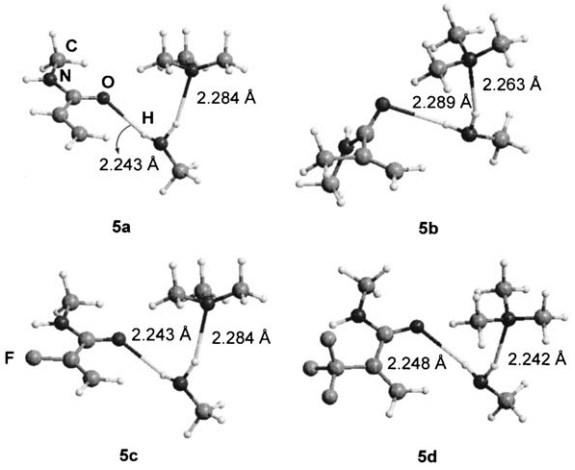

Figure 2. Starting ternary complexes on the potential energy surface.

Table 2. Energies of the stationary points located for the Michael additions of methylamine to acrylamides **4a**–**d**.

Stationary point	Relative energy[a]	Relative energy[b]
5a	−10.5	0.0
5b	−4.7	0.0
5c	−16.5	0.0
5d	−10.9	0.0
6a-*trans*	18.2	28.7
7	16.3	26.8
6a-*cis*	7.7	18.2
8a	−2.3	8.2
6b-*cis*	14.0	16.3
6c-*cis*	7.9	24.4
6d-*cis*	−4.5	6.3
8b	0.4	5.1
8c	−1.2	−15.3
8d	−9.5	1.4
9a	20.3	30.8
9b	24.8	29.5
9c	17.3	33.7
9d	5.1	16.0
10a	−27.9	−17.4
10b	−20.0	−15.3
10c	−26.7	−10.3
10d	−26.4	−15.5

[a] Relative energy [kcal mol^{-1}] with respect to isolated reactants. [b] Relative energy [kcal mol^{-1}] with respect to ternary complexes **5**.

leading to the formation of a C–N bond. However, we reached different results depending on the conformation of the Michael acceptor (Figure 3).

Thus, when the Michael acceptor **4a** (R = H) reacts in the *s-trans* conformation, the transition structure **6a**-*trans* is located. This transition structure shows an imaginary vibrational normal mode corresponding to the formation of the N–C_β bond leading to the zwitterionic intermediate **7**. The transition structure **6a**-*trans* and intermediate **7** are 18.2 and 16.3 kcal mol^{-1} above the reactants, respectively. In the intermediate **7** the N–C_β bond is fully formed, but no hydrogen atom is transferred from the nitrogen of the nucleophile

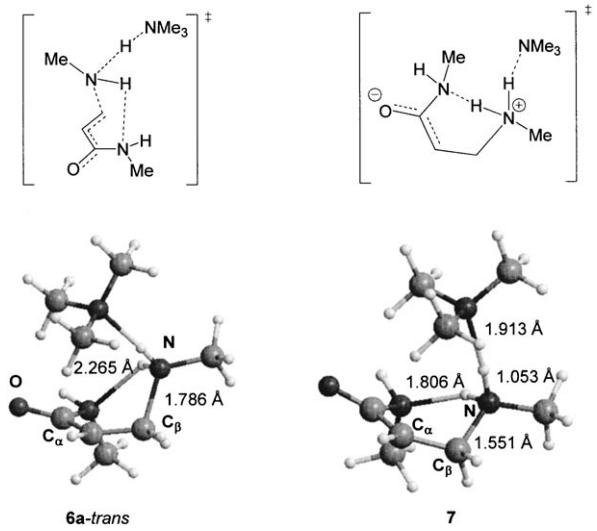

Figure 3. Transition structures for nucleophilic additions of methylamine to s-*trans*- and s-*cis*-Michael acceptor **4a**, together with zwitterionic intermediate **7**.

(methylamine), either to the C_α or to the oxygen of the Michael acceptor (Figure 3).

On the other hand, when the Michael acceptor reacts in the *s-cis* conformation, this results in a different reaction pathway. Thus, in the case of the acrylamide **4a**, the transition structure **6a**-*cis* shows the trimethylamine hydrogen-bonded to one of the hydrogens of the methylamine NH_2 grouping, and in addition, a hydrogen bond between the carbonyl group and one of the hydrogens of the methylamine (Figure 4).

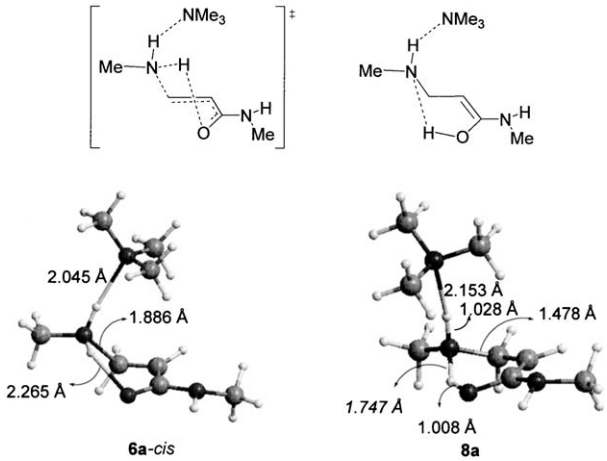

Figure 4. Transition structure for the nucleophilic addition of the amine to the s-*cis* conformation of the Michael acceptor **4a**, together with amide–enol intermediate **8a**.

The normal mode associated with the imaginary vibrational frequency of **6a**-*cis* corresponds mainly to the stretching of the forming N–C_β bond, with no significant contribu-

 © 2007 Wiley-VCH Verlag GmbH & Co. KGaA, Weinheim

tion from the N–H stretching.[16] According to the IRC calculations, the enol–amide intermediate **8a** is formed.

The reaction barrier for the nucleophilic addition of the methylamine to the acrylamide **4a** to form **8a** is substantially lowered in relation to the process in which the Michael acceptor reacts in the s-*trans* conformation (Table 2). In the intermediate **8a**, one of the hydrogens of the nucleophile is transferred to the oxygen of the Michael acceptor, and forms a short hydrogen bond (1.747 Å) with the nitrogen of the methylamine fragment (Figure 4). According to these results, the addition of the methylamine to the *s-cis* conformer of the Michael acceptor **4a** could be considered a concerted, yet highly asynchronous, reaction.

While the two reaction pathways each involve a charge separation (due to the charge transfer from the amine to the electrophilic Michael acceptor), in the case of the addition to the *s-cis* conformer of **4a** an intramolecular hydrogen bond is present in the corresponding transition structure **6a**-*cis* (Figure 4), which is stabilized as a result, relative to **6a**-*trans*. The role of intramolecular hydrogen bonds in Michael additions for reactions between enamine derivatives and nitroethylene has been described before.[17,18] In addition, it should be noted that an analysis of the magnitude of the charge transfer from the methylamine-triethylamine fragment to the Michael acceptor moiety in **6b-***cis* and **6b-***trans*, based on the Mulliken charges, shows that in the case of the transition structures **6b-***trans* the charge transfer is greater than in the transition structure **6b-***cis*. This is reflected in the values of the dipole moments of the two transition structures: 4.152 D in **6b-***cis* versus 7.126 D in **6b-***trans*.

It is interesting to note that the distance between the N–H hydrogen of the amide grouping and one of the fluorine atoms of the Tfm grouping in transition structure **6d**-*cis* is very short (2.121 Å). This interaction, which is absent in all the other transition structures located and seems to be electrostatic in nature,[19] might contribute in maintaining the rigidity of this moiety, a feature that can be crucial in the control of the stereoselectivity of the reaction.

The Michael reactions of acrylamides **4b**, **4c**, and **4d** (see Figure 1), in the *s-cis* conformation, were studied at the same level of theory, resulting in potential energy surfaces quite similar to the one found in the case of **4a**. In Figure 5, the transition structures **6b**-*cis*, **6c**-*cis*, and **6d**-*cis*, located for the nucleophilic addition, and the corresponding enol–amide intermediates **8b–d**, formed in the reaction, can be found.

Another interesting result that can be seen in the previous data is the great difference in the reactivities of the Michael acceptors **4a–c** and **4d**. The presence of the trifluoromethyl group thus stabilizes the corresponding transition structure (**6d**-*cis*) extraordinarily for the nucleophilic addition, resulting in a barrier significantly lower than in the cases of Michael acceptors **4a–c** (Table 2). The difference in the reactivities of the Michael acceptors **4a–d** is also reflected in the lengths of the forming N–C_β bonds in the corresponding transition structures: **6c-***cis* proves to be a late transition structure in comparison with **6d-***cis* (see Figure 5). This behavior is in full agreement with the experimental results showing that the acrylamide acceptors of type **4a–c** are unreactive in this aza-Michael process, while the reaction with the Tfm-containing system takes place very easily. This situation can be interpreted in terms of Frontier Molecular Orbital theory,[20] by considering the energies[21] of the LUMOs of the Michael acceptors.[22] The Tfm group greatly stabilizes the LUMO of **4d**, relative to the other acrylamide derivatives, making this Michael acceptor more electrophilic than in the case of the methyl group or the hydrogen.[23] On the other hand, the LUMO of the fluoroacrylamide **4c** is lowered, but not sufficiently to make this compound a good Michael acceptor, as can be seen from the values of the activation energy for the nucleophilic addition (transition structure **6c**-*cis*, and Table 2); indeed, the corresponding fluoroacrylamide proved to be unreactive in this process.

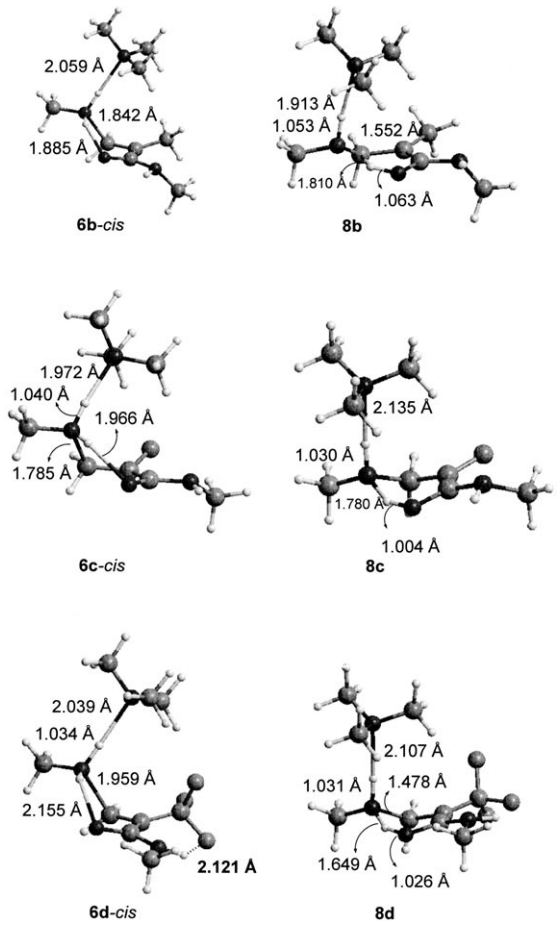

Figure 5. Transition structures for the addition to the *s-cis* Michael acceptors and neutral enol–amide intermediates.

The potential energy surface for the nucleophilic addition to the *s-cis* Michael acceptor was also studied at a higher level of theory. The stationary points for the reaction pathway in the addition of methylamine to **4a** (see Figure 1), both in the presence and in the absence of ammonia as the catalytic base, were located at the MP2/6-31G* level of

 © 2007 Wiley-VCH Verlag GmbH & Co. KGaA, Weinheim

theory (see Supporting Information section, Figure S1). The results of this study are similar to those obtained with DFT.

Intramolecular hydrogen transfer in the enol–amide intermediates 8: After the formation of the enol–amide intermediates **8**, we located the transition structures for the hydrogen transfer from the nucleophile moiety to the α-carbon atom. This is an important step because it is at this point that the new stereogenic center is formed. The Michael adducts **10** (Figure 8) are formed by hydrogen transfer from the nitrogen of the nucleophile to the α-carbon. The transition structures for this step are shown in Figure 6.

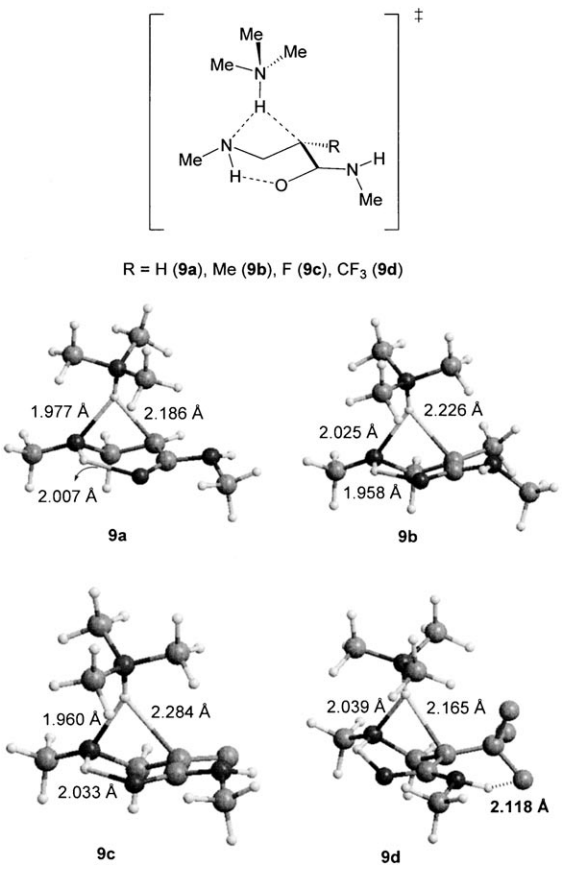

Figure 6. Transition structures for the intramolecular hydrogen transfer.

The hydrogen atom that is being transferred is simultaneously bonded to the trimethylamine fragment, to the nitrogen of the nucleophile, and to the α-carbon atom. There is also a hydrogen bond between the nitrogen of the nucleophile and the oxygen of the carbonyl in each of the four transition structures located. Analysis of the normal mode associated with the imaginary frequency of the transition structures **9a–d** shows that the trimethylammonium fragment acts as a carrier of the hydrogen between the nitrogen and the carbon atoms. These structures are quite similar to those found by Houk and co-workers for enol–keto tautomerizations.[24]

Also, as indicated before (see Figure 5, **6d**-*cis*), an electrostatic interaction exists between the hydrogen of the CON–H grouping and one of the fluorine atoms. The distance between the hydrogen and fluorine atoms is 2.118 Å.[19]

As can be observed from the data in Table 2 and Figure 8, the Tfm group reduces the activation energy for the intramolecular hydrogen transfer step, relative to the cases of other Michael acceptors. This effect could be explained by taking account of the fact that the interaction between the Michael acceptor moiety and the trimethylammonium fragment in the transition structures for the hydrogen transfer is mainly electrostatic. Consequently, the Michael acceptor moiety can be regarded as an enolate species. In this situation, the presence of the strongly electron-withdrawing Tfm group causes a greater stabilization of transition structure **9d** (Figure 6) than in the cases of **9a–c**, in which there is no stabilizing group.

Catalytic effect of the base: Moreover, the trimethylamine also acts as a catalyst for the intramolecular hydrogen transfer from the nucleophilic nitrogen to C_α in the Michael acceptor, also playing a catalytic role in the addition step. Also in the uncatalyzed reaction, the Michael acceptor and methylamine form a binary complex **11**, and the addition to C_β in the unsaturated system takes place through a transition structure **12**, very similar to those found in the case of the catalyzed reaction, resulting in the enol–amide intermediate **13**. However, the activation barrier for the addition step of methylamine to **4d**, in the absence of trimethylamine, amounts to 12.0 kcal mol^{-1}, which is twice the corresponding value for the activation barrier of the Me_3N-catalyzed reaction (Figure 7). This effect is also reflected in the

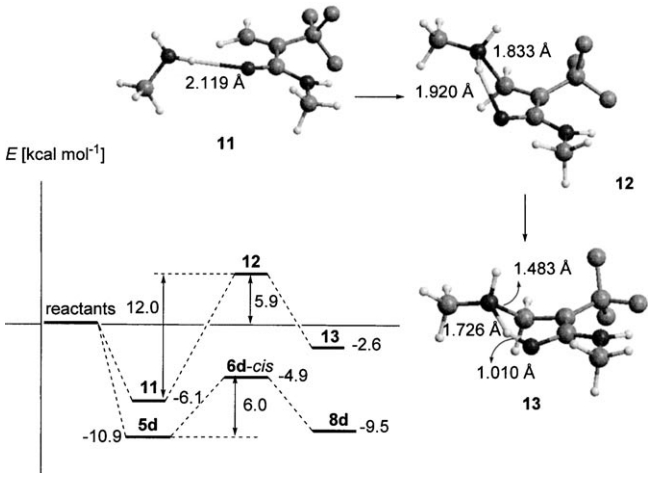

Figure 7. Uncatalyzed addition of methylamine to **4d** (bottom) in comparison with the Me_3N-catalyzed reaction (top).

fact that **12** is a late transition structure (R[N–C_β] = 1.833 Å) in relation to the transition structure **6d**-*cis* (see Figure 5) for the nucleophilic addition in the catalyzed reaction (R[N–C_β] = 1.959 Å).

 © 2007 Wiley-VCH Verlag GmbH & Co. KGaA, Weinheim

The geometries of the transition structures for the hydrogen transfer step also help to explain the different results obtained when triethylamine is used as base, instead of DABCO or trimethylamine.[12] Because of the great steric congestion in the transition structure **9d** (Figure 6), the use of a base with higher steric requirements, such as triethylamine (relative to DABCO or trimethylamine), will result in a severe distortion of the transition structure, which in turn will cause a decrease in the stereoselection.

According to the calculations, the addition of a primary amine derivative to the Michael acceptors **4** is a stepwise process. The first step corresponds to the formation of the C_β–N bond in a reaction leading to an enol–amide intermediate, undergoing an intramolecular hydrogen transfer step from the nitrogen to the C_α carbon atom, to generate the new stereogenic center. The trimethylamine acts as catalyst in the two steps. The different reaction pathways are compared in Figure 8, and it can be seen that the second step is rate-determining.

The data shown in Figure 8 and Table 2 indicate that the increased reactivity shown by the trifluoromethylacrylamide acceptor **4d**, relative to the analogous systems **4a–c**, is related to the very low barriers both for the nucleophile addition step and for the intramolecular hydrogen transfer. This effect can be specifically attributed to the presence of the Tfm group, which is critical for the reaction, as discussed in the previous analysis of the Khon–Sham frontier orbitals.

Origin of the stereoselectivity: The stereogenic center formed in the aza-Michael addition of an amine derivative to the acrylamide acceptor **4d** is created in the second step of the reaction: namely, the intramolecular hydrogen transfer from the nucleophile nitrogen to the C_α carbon atom. In order to understand the factors underlying the stereocontrol in this step, we studied the aza-Michael reactions of acceptor (*S*)-**2l** with the alanine-derived amines (*S*)-**1l** and (*R*)-**1l** to give the Michael adducts **3l** and **3m** (see Scheme 3 and Table 1, entries 13 and 14).

In the first case, we have pair-matched reactants, while the second reaction is an example of a mismatched pair reaction. According to the experimental data shown in Table 1, the stereoselection is notably greater in the case of the pair-matched reaction. In addition, the reaction between the most sterically demanding Michael acceptor (*S*)-**2c**, bearing an isopropyl group, and the amine (*S*)-**1c**, leading to the product **3c** (Table 1, entry 3), was studied in order to

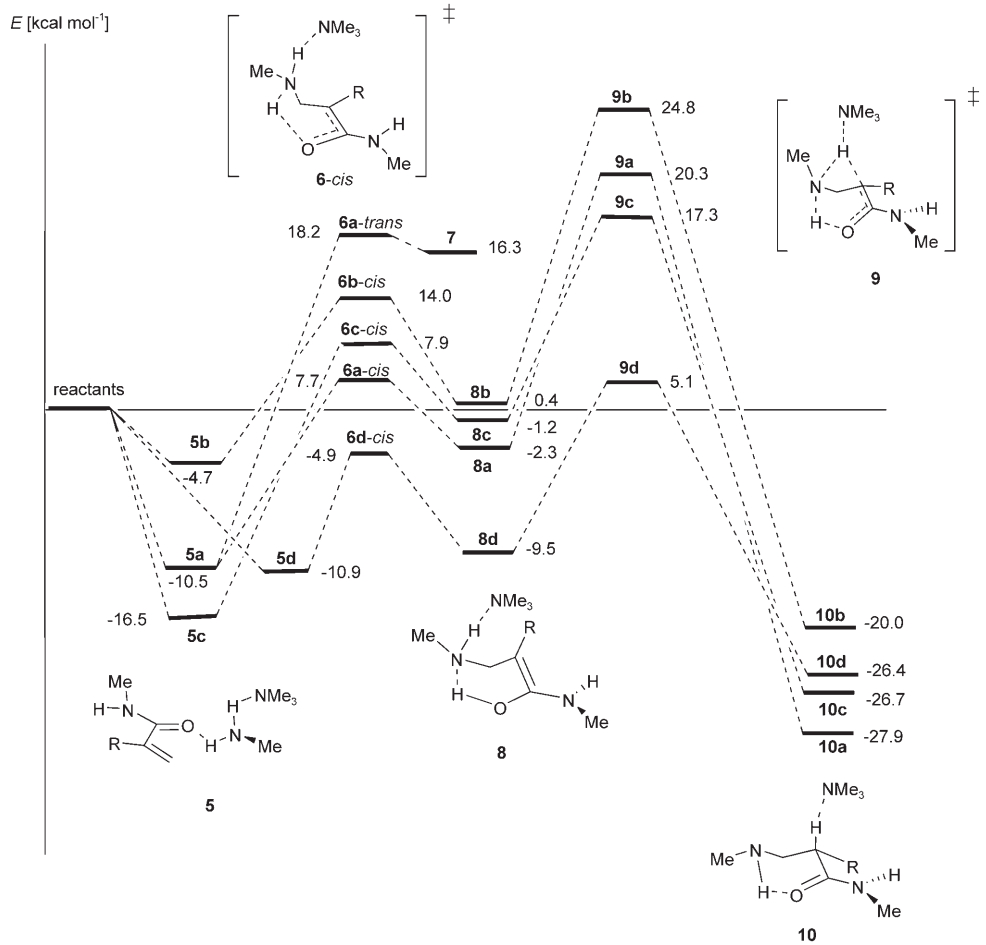

Figure 8. Reaction pathways for the addition of methylamine to the Michael acceptors **4a–d**.

 © 2007 Wiley-VCH Verlag GmbH & Co. KGaA, Weinheim

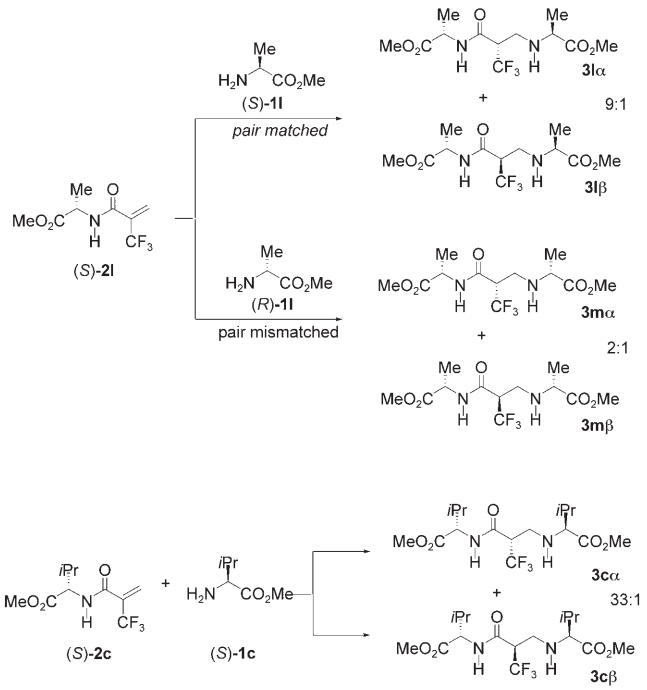

Scheme 3. Influence of the steric demand and the absolute configuration of the reactants on the aza-Michael reaction.

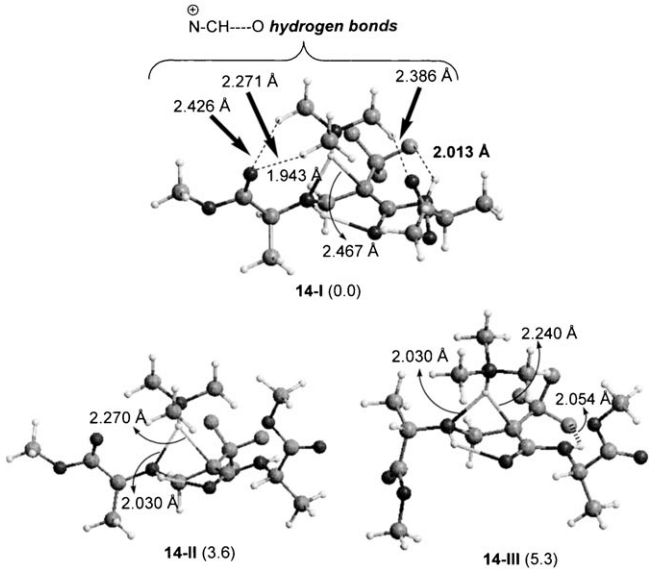

Figure 9. The three saddle points located for the intramolecular hydrogen transfer step in the reaction between (*S*)-**2l** and (*S*)-**1l**. Relative energy in kcal mol^{-1}.

shed light on the steric effects on the asymmetric induction. In this case, the reaction stereoselectivity showed a great increase when compared with the previous reactions of the methyl-containing reactants (entries 13 and 14 vs 3, Table 1).

All the stationary points for the reaction between (*S*)-**2l** and (*S*)-**1l** were located (see Supporting Information). The potential energy surface is qualitatively similar to that found for the simple Tfm-acrylamide model **4d**.

In spite of the observed similarities, however, we found three different saddle points (**14-I**, **14-II**, and **14-III**; see Figure 9) for the intramolecular hydrogen transfer step, leading to the major diastereoisomer **3lα** (see Scheme 3). There are significant differences in the relative positions of the ester groupings in the three cases. Also, the three saddle points differ in energy, **14-I** being the most stable one, by 3.6 and 5.3 kcal mol^{-1} respectively, in relation to **14-II** and **14-III**.

One of the keys to understanding of these differences lies in the interactions between the carbonyl groups of the esters and the hydrogens of the partially positively charged trimethylammonium fragment. The oxygen atoms of the carbonyl groups are able to form hydrogen bonds with the hydrogens of the Me_3HN^+ fragment, thus stabilizing its cationic character.

The role of this type of O···HCN$^+$ hydrogen bonding has previously been analyzed by Houk and co-workers,[25] while its influence on the control of the stereoselectivity of Diels–Alder reactions has also been described.[26] According to these results, **14-I** is the true transition structure for the formation of **3lα**. Moreover, the transition structure **15-I**, leading to the diastereoisomer **3lβ**, was located (Figure 10).

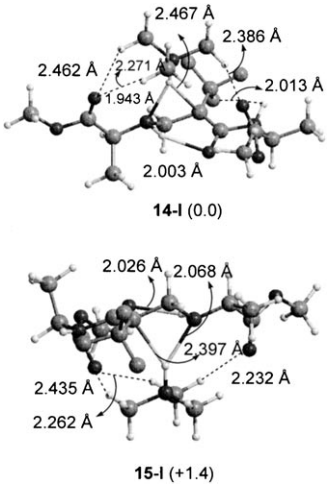

Figure 10. Transition structures leading to the diastereoisomers **3lα** and **3lβ**, respectively. Relative energy in kcal mol^{-1}.

As can be seen in Figure 10, this transition structure is 1.4 kcal mol^{-1} less stable than **14-I**, thus indicating that diastereoisomer **3lα** will be formed preferentially.

It should be noted that according to the experimental data,[12] the polarity of the solvent strongly influences the diastereomeric ratio of the reaction. The best stereocontrol is achieved with the least polar solvent (CCl_4). This result can be understood if it is taken into account that the presence of solvents able to form intermolecular hydrogen bonds disrupts the network of intramolecular hydrogen bonds, previously described and depicted in Figures 9 and 10.

 © 2007 Wiley-VCH Verlag GmbH & Co. KGaA, Weinheim

It is interesting to note that the difference between the transition structures leading to the two possible diastereoisomers is reduced in the case of the *mismatched* approach (Figure 11), in good agreement with the experimental results. Thus, in the reaction between (*S*)-**2l** and (*R*)-**1l** (Scheme 3), the diastereoisomer ratio is reduced to 2:1. In this case the transition structure **16**, leading to the major stereoisomer **3mα**, is only 0.8 kcal mol^{-1} more stable than **17**, which leads to **3mβ** (Figure 11).[27]

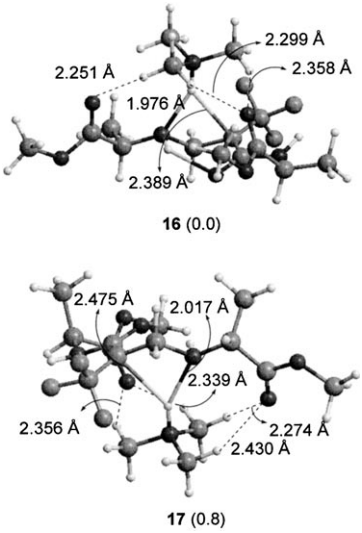

Figure 11. Transition structures **16** and **17** for the *mismatched* reaction. Relative energy in kcal mol^{-1}.

In the case of the reaction of the valine-derived Michael acceptor (*S*)-**2c** (Scheme 3 and Table 1, entry 3), the stereoselectivity is significantly higher (33:1). The presence of the two isopropyl groups, both in the attacking nucleophile and the Michael acceptor, contributes to the increase in the degree of stereocontrol. The transition structures corresponding to the two possible modes of intramolecular hydrogen transfer (**18** and **19**, Figure 12) were located.

The energy difference between the two diastereomeric transition structures (4.3 kcal mol^{-1}) is now substantially greater than in the case of the reaction of Michael acceptor (*S*)-**2l**, in good agreement with the experimental observations.

In order to understand the origin of the stereoselectivity in the intramolecular hydrogen transfer step properly, three common factors have to be taken into account: a) the presence of a hydrogen bond between the carbonyl oxygen and the NH group of the attacking nucleophile, b) the strong interaction between one of the fluorine atoms of the Tfm group and the NH of the Michael acceptor, which forces an almost planar conformation of the CF_3-C-C(=O)-N-H fragment, and c) the interactions between the hydrogens of the trimethylammonium fragment and some of the carbonyl groups of the esters. The important role played by these hydrogen bonds in the stereocontrol of the reaction is in good agreement with the experimental observation showing that the stereoselectivity strongly decreases if the reaction is carried out in a solvent capable of forming hydrogen bonds with the reactants.

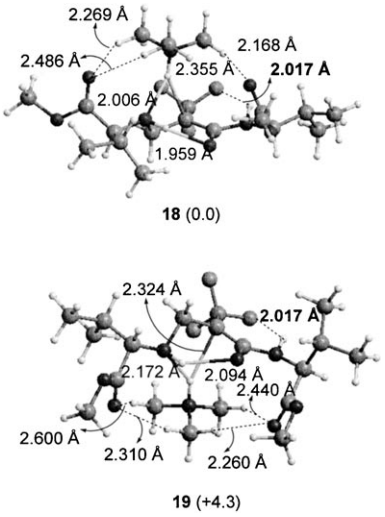

Figure 12. Diastereoisomeric transition structures for the intramolecular hydrogen transfer in the reaction between (*S*)-**2c** and (*S*)-**1c**. Relative energy in kcal mol^{-1}.

In addition to the previous considerations, there also needs to be consideration of i) whether the steric effects of the two stereocenters on the stereocontrol are additive, and ii) if this is the case, what is the main factor determining the differences in energy between the transition structures leading to the diastereoisomers?

We have analyzed the differences in energy (ΔE) of the diastereomeric pairs of transition structures for the reactions of the Michael acceptors (*S*)-**2l** and (*S*)-**2c** with the amines (*S*)-**1l**, (*R*)-**1l**, and (*S*)-**1c** (see Scheme 3), and have tried to correlate them with the geometries of the systems. It seems that the values of two dihedrals ω_1 and ω_2 (see Figure 13), which define the relative positions of the two chiral centers in the transition structures, influence the differences in energy (ΔE) between the diastereomeric transition structures (Table 3).

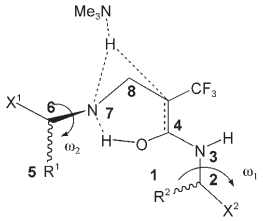

R^1= Me, *i*Pr; X^1= X^2= CO_2Me
R^2= Me, *i*Pr; X^1= X^2= CO_2Me

Figure 13. Dihedral angles ω_1 and ω_2 discussed in Table 3.

From the data in Table 3 it is possible to envisage a kind of correlation: in the two reactions—matched and mismatched—the more stable transition structure is the one with the dihedral ω_1, the one governing the relative position of the stereogenic center of the Michael acceptor moiety (Figure 13), closer to 180°. This spatial position decreases the steric interactions, while in the case of ω_1 having a low value, a more sterically *gauche* disposition is present (see Figures 14 and 15, and Supporting Information).

 © 2007 Wiley-VCH Verlag GmbH & Co. KGaA, Weinheim

Table 3. Correlation between the dihedral angles in the transition structures and the relative energy ΔE (in kcal mol^{-1}).

Reactants[a]	TS[b]	Products[b]	$\lvert\omega_1\rvert$ [°]	$\lvert\omega_2\rvert$ [°]	ΔE
(*S*)-**2l** + (*S*)-**1l**	**14-I** [*SSS*]	**3lα** [*SSS*]	172	89	0.0
(*S*)-**2l** + (*S*)-**1l**	**15-I** [*SRS*]	**3lβ** [*SRS*]	70	66	+1.4
(*S*)-**2l** + (*R*)-**1l**	**16** [*SSR*]	**3mα** [*SSR*]	175	62	0.0
(*S*)-**2l** + (*R*)-**1l**	**17** [*SRR*]	**3mβ** [*SRR*]	70	86	+0.8
(*S*)-**2c** +(*S*)-**1c**	**18** [*SSS*]	**3cα** [*SSS*]	169	138	0.0
(*S*)-**2c** +(*S*)-**1c**	**19** [*SRS*]	**3cβ** [*SRS*]	71	61	+4.3

[a] Michael acceptor + nucleophilic amine. [b] The first letter between the brackets corresponds to the absolute configuration of the stereogenic center of the Michael acceptor, the second one to the stereogenic center generated in the reaction, and the third one to the nucleophilic amine.

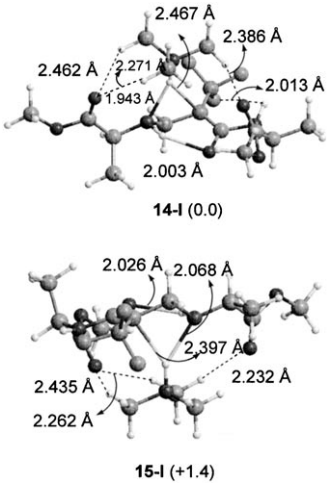

Figure 15. Dihedral angle ω_2 in the diastereomeric transition structures **14-I** and **15-I**.

Figure 14 shows that the *anti* and *gauche* dispositions of groups R and R^2 in the transition structures are the result of different steric interactions, which thus influence the relative energies of the two diastereomeric transition structures for the intramolecular hydrogen transfer.

On the other hand, the dihedral ω_2, which governs the relative position of the stereogenic center of the nucleophile moiety (Figure 13) seems to modulate the effect of ω_1; thus, as ω_2 has a lower value for the major diastereoisomeric transition structure, ΔE increases, and consequently the diastereoisomeric ratio is reduced, as can be seen in the case of the mismatched reaction (see Figure 15 and Supporting Information).

Our preliminary results point to a more general scheme: the effects of the stereogenic centers of the Michael acceptor and the nucleophile can be considered independent each from the other, as well as additives. In addition, each chiral center induces the same configuration in the newly generated center, the influence of the stereogenic center in the Michael acceptor being greater than that of the amine. In order to test this model, a new computational experiment was carried out. In this experiment, the presence or the absence of one of the stereogenic centers in the reaction partners is controlled.[28]

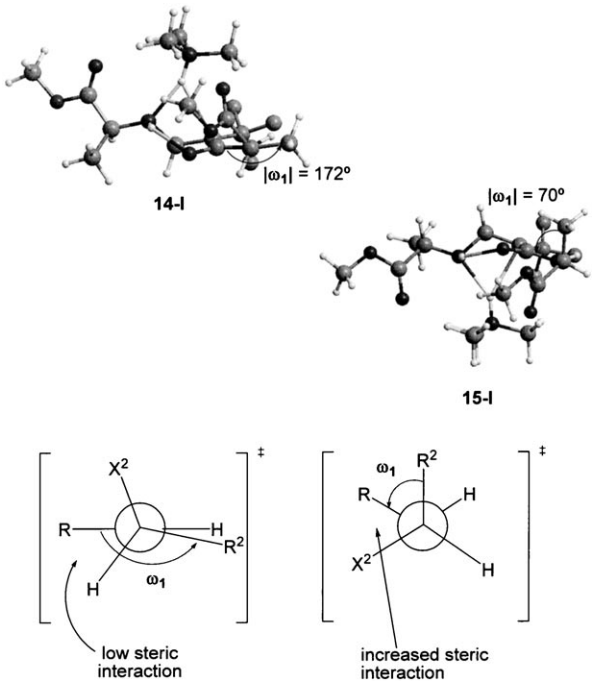

Figure 14. Dihedral angle ω_1 and different steric interactions in transition structures **14-I** and **15-I**.

Conclusions

We report the mechanistic analysis of a new type of aza-Michael reaction, involving trifluoromethyl-containing Michael acceptors. The reactions take place with high degrees of stereocontrol, leading to partially modified Ψ-[$NHCH_2$]retropeptides incorporating a hydrolytically stable trifluoroalanine mimic. According to the theoretical study, carried out with density-functional theory methods, the reaction is a two-step process, with an initial nucleophilic attack of the amine on the acceptor double bond, in which a neutral enol–amide intermediate is formed.

The second step corresponds to an intramolecular hydrogen transfer catalyzed by the amine present in the reaction medium. At the same time, a new chiral center is formed. The role of the Tfm group appears to be critical both in the reactivity of the Michael acceptor and in the control of the reaction stereoselectivity. The Tfm grouping makes the Michael acceptor more electrophilic, dramatically reducing the activation barrier of the reaction. In addition, the electrostatic interaction between one of the fluorine atoms of the CF_3 fragment with the hydrogen of the amide influences the conformation of the transition structure.

 © 2007 Wiley-VCH Verlag GmbH & Co. KGaA, Weinheim

On the other hand, the $N^+CH{-}O$ hydrogen bonds are critical in maintaining the rigidity of the transition structure. This effect, coupled with the steric hindrance of the substituents in the stereogenic centers of the nucleophile and the Michael acceptor, determines the high degree of stereocontrol observed.

Experimental Section

General methods: Reactions were carried out under nitrogen unless otherwise indicated. The solvents were purified prior to use: CH_2Cl_2 and CCl_4 were distilled from calcium hydride. All reagents were used as received. The reactions were monitored with the aid of thin-layer chromatography (TLC) on 0.25 mm E. Merck precoated silica gel plates. Visualization was carried out with UV light and aqueous ceric ammonium molybdate solution or potassium permanganate stain. Flash column chromatography was performed with the indicated solvents on silica gel 60 (particle size 0.040–0.063 mm). Melting points were measured on a Büchi B-540 apparatus and are uncorrected. Optical rotations were measured on a Jasco P-1020 polarimeter. ^1H, ^{13}C, and ^{19}F NMR spectra were recorded on a 300 MHz Bruker AC 300 spectrometer and a 400 MHz Bruker Avance instrument. Chemical shifts are given in ppm (δ), referenced to the residual proton resonances of the solvents or fluorotrichloromethane in ^{19}F NMR experiments. Coupling constants (J) are given in Hertz (Hz). The letters m, s, d, t, and q stand for multiplet, singlet, doublet, triplet, and quartet, respectively. The letters br indicate that the signal is broad. High-resolution mass spectra were carried out on a VGmAutospec instrument (VG Analytical, Micromass Instruments) by the Universidad de Valencia Mass Spectrometry Service.

Preparation of fluorinated acceptors 2

Benzyl (*S*)-4-methyl-2-(2-trifluoromethylacryloylamino)pentanoate (2a): This compound was prepared as follows: A solution of (*S*)-leucine benzyl ester (**1a**, 100 mg, 0.25 mmol) and *sym*-collidine (0.06 mL, 0.5 mmol) in methylene chloride (3 mL) was added dropwise at 0 °C to a solution of trifluoromethylacryloyl chloride (44 mg, 0.28 mmol) in CH_2Cl_2 (1 mL). The reaction mixture was stirred at this temperature until TLC revealed total consumption of the starting material (1 h). The crude mixture was then quenched with HCl (5%, 15 mL) and extracted with CH_2Cl_2 (3× 15 mL). The combined organic layers were dried over anhydrous sodium sulfate, and solvents were removed under reduced pressure. The crude reaction mixture was subjected to flash chromatography (*n*-hexane/ethyl acetate 7:3) to afford **2a** (81 mg, 95%) as a yellow oil. $[\alpha]_D^{25} = -16.7°$ (c = 1.0 in $CHCl_3$); ^1H NMR (300 MHz, $CDCl_3$): δ = 0.84 (d, J = 2.0 Hz, 3H), 0.86 (d, J = 2.0 Hz, 3H), 1.49–1.70 (m, 3H), 4.65–4.72 (m, 1H), 5.07 (d, J = 12.2 Hz, 1H), 5.12 (d, J = 12.2 Hz, 1H), 6.16 (q, J(H,F) = 1.3 Hz, 1H), 6.36 (d, J = 7.1 Hz, 1H), 6.44 (q, J(H,F) = 1.5 Hz, 1H), 7.26 ppm (s, 5H); ^{13}C NMR (75.5 MHz, $CDCl_3$): δ = 22.3 (CH_3), 23.0 (CH_3), 25.2 (CH), 41.6 (CH_2), 51.7 (CH), 67.7 (CH_2), 122.4 (C_q, ^1J(C,F) = 273.1 Hz), 128.6 (CH), 128.8 (CH), 129.0 (CH), 129.9, (C_q, ^3J(C,F) = 5.7 Hz), 134.0 (C_q, ^2J(C,F) = 31.0 Hz), 135.5 (C), 160.9 (C), 172.5 ppm (C); ^{19}F NMR (282.4 MHz, $CDCl_3$): $\delta = -64.2$ ppm (s, 3F); HRMS: m/z: calcd for $C_{17}H_{20}F_3NO_3$: 343.1395; found: 343.1390 $[M]^+$.

***N*-[(1*S*)-1-Naphthalen-1-yl-ethyl]-2-trifluoromethylacrylamide (2g)**: This compound was prepared as follows: A solution of (*S*)-α-methylnaphthylamine (**1e**, 490 mg, 2.86 mmol) and *sym*-collidine (0.37 mL, 2.86 mmol) in CH_2Cl_2 (16 mL) was added dropwise at 0 °C to a solution of trifluoromethylacryloyl chloride (500 mg, 3.15 mmol) in CH_2Cl_2 (8 mL). The reaction mixture was stirred at this temperature until TLC revealed total consumption of the starting material (2 h). The crude mixture was then quenched with saturated ammonium chloride (15 mL) and extracted with CH_2Cl_2 (3×15 mL). The combined organic layers were dried over anhydrous sodium sulfate, and solvents were removed under reduced pressure. The crude reaction mixture was subjected to flash chromatography (*n*-hexane/ethyl acetate 5:1) to afford **2g** as a white solid (419 mg, 50%). M.p. 135–137 °C; $[\alpha]_D^{25} = -63.1°$ (c = 0.9 in $CHCl_3$); ^1H NMR (300 MHz, $CDCl_3$): δ = 1.65 (d, J = 6.8 Hz, 3H), 5.88–5.97 (m, 1H), 6.09 (br s, 1H), 6.14 (q, J(H,F) = 1.3 Hz, 1H), 6.44 (q, J(H,F) = 1.5 Hz, 1H), 7.36–7.50 (m, 4H), 7.51–7.82 (m, 2H), 7.99 ppm (d, J = 8.1 Hz, 1H); ^{13}C NMR (100 MHz, $CDCl_3$): δ = 20.7 (CH_3), 45.5 (CH), 122.1 (C_q, ^1J(C,F) = 271.2 Hz), 122.5 (CH), 123.0 (CH), 125.2 (CH), 125.9 (CH), 126.2 (CH), 126.6 (CH), 128.6 (CH), 129.2 (C_q, ^3J(C,F) = 5.5 Hz), 130.9 (C), 133.9 (C), 133.9 (C_q, ^2J(C,F) = 30.4 Hz), 137.4 (C), 159.8 ppm (C); ^{19}F NMR (282.4 MHz, $CDCl_3$): $\delta = -64.2$ ppm (s, 3F); HRMS: m/z: calcd for $C_{16}H_{14}F_3NO$: 293.1027; found: 293.1054 $[M]^+$.

General procedure for the preparation of Michael adducts 3: Amine **1** (0.22 mmol) was added at 0 °C to a stirred solution of **2** (0.22 mmol) in CCl_4 (5 mL). DABCO (0.22 mmol) was then added, and the mixture was stirred for 2 h at room temperature. The reaction was monitored by thin-layer chromatography (TLC). The solvent was removed under vacuum, yielding a diastereoisomeric mixture of **3α/3β** which was in turn separated by flash chromatography with silica gel as stationary phase to afford the corresponding adducts **3** as white solids.

Benzyl (*S*)-2-{(*S*)-2-[((*S*)-1-benzyloxycarbonyl-3-methyl-butylamino)-methyl]-3,3,3-trifluoropropionylamino}-4-methylpentanoate (3aα): This compound was prepared by the general procedure described above, starting from **2a** (30 mg, 0.08 mmol) and (*S*)-**1a** (31 mg, 0.08 mmol), to afford **3aα** (46 mg, 0.08 mmol) as a white solid after flash chromatography (*n*-hexane/diisopropyl ether 2:1) on deactivated silica gel (2% Et_3N in *n*-hexane); yield 95%; m.p. 53–56 °C; $[\alpha]_D^{25} = +2.4°$ (c = 0.3 in $CHCl_3$); ^1H NMR (300 MHz, $CDCl_3$): δ = 0.77–0.85 (m, 12H), 1.18 (s, 1H), 1.30–1.42 (m, 2H), 1.44–1.62 (m, 4H), 2.83–3.00 (m, 3H), 3.24 (dd, J_1 = 7.9 Hz, J_2 = 6.4 Hz, 1H), 4.54–4.62 (m, 1H), 5.03 (d, J = 12.2 Hz, 2H), 5.11 (d, J = 10.9 Hz, 2H), 7.27 (d, J = 1.3 Hz, 5H), 7.29 (d, J = 1.1 Hz, 5H), 7.34 ppm (d, J = 7.7 Hz, 1H); ^{13}C NMR (75.5 MHz, $CDCl_3$): δ = 21.7 (CH_3), 22.0 (CH_3), 22.7 (CH), 24.8 (CH), 40.9 (CH_2), 42.5 (CH_2), 44.8 (CH_2), 50.7 (C_q, ^2J(C,F) = 23.6 Hz), 51.0 (CH), 60.5 (CH), 66.7 (CH_2), 67.1 (CH_2), 124.3 (C_q, ^1J(C,F) = 281.0 Hz), 128.2 (CH), 128.3 (CH), 128.4 (CH), 128.4 (CH), 128.5 (CH), 135.2 (C), 135.4 (C), 165.9 (C), 172.5 (C), 175.7 ppm (C); ^{19}F NMR (282.4 MHz, $CDCl_3$): $\delta = -67.0$ ppm (d, J(H,F) = 8.2 Hz, 3F); HRMS: m/z: calcd for $C_{30}H_{39}F_3N_2O_5$: 565.2889; found: 565.2882 $[M+H]^+$.

Benzyl (*S*)-2-{(*S*)-2-[((*S*)-1-benzyloxycarbonyl-2-methylpropylamino)-methyl]-3,3,3-trifluoropropionylamino}-3-methylbutanoate (3bα): This compound was prepared by the general procedure described above, starting from **2b** (30 mg, 0.09 mmol) and (*S*)-**1b** (22 mg, 0.09 mmol), to afford **3b**α (45 mg, 0.08 mmol) as a white solid after flash chromatography (*n*-hexane/diisopropyl ether 1:3) on deactivated silica gel (2% Et_3N in *n*-hexane); yield 95%; m.p. 48–50 °C; $[\alpha]_D^{25} = +11.4°$ (c = 1.0 in $CHCl_3$); ^1H NMR (300 MHz, $CDCl_3$): δ = 0.76–0.87 (m, 12H), 1.79 (s, 1H), 1.82–1.91 (m, 1H), 2.08–2.18 (m, 1H), 2.90–3.02 (m, 4H), 4.56 (dd, J_1 = 8.6 Hz, J_2 = 4.7 Hz, 1H), 5.01–5.13 (m, 4H), 7.26 (s, 5H), 7.28 ppm (s, 5H); ^{13}C NMR (75.5 MHz, $CDCl_3$): δ = 17.4 (CH_3), 18.0 (CH_3), 18.9 (CH_3), 19.0 (CH_3), 30.8 (CH), 31.5 (CH), 45.4 (C_q, ^3J(C,F) = 2.2 Hz), 51.0 (C_q, ^2J(C,F) = 25.3 Hz), 57.3 (CH), 66.6 (CH_2), 67.0 (CH_2), 67.7 (CH_2), 124.3 (C_q, ^1J(C,F) = 280.0 Hz), 128.3 (CH), 128.3 (CH), 128.4 (CH), 128.5 (CH), 128.5 (CH), 135.1 (C), 135.4 (C), 166.1 (C), 171.5 (C), 175.1 ppm (C); ^{19}F NMR (282.4 MHz, $CDCl_3$): $\delta = -67.1$ ppm (d, J(H,F) = 8.2 Hz, 3F); HRMS: m/z: calcd for $C_{28}H_{35}F_3N_2O_5$: 537.2576; found: 537.2561 $[M+H]^+$.

***tert*-Butyl (*S*)-3-methyl-2-[(1*S*)-3,3,3-trifluoro-2-((S)-1-phenylethylcarbamoyl)propylamino]butanoate (3eα)**: This compound was prepared by the general procedure described above, starting from **2e** (100 mg, 0.4 mmol) and (*S*)-**1d** (86 mg, 0.4 mmol), to afford **3eα** (128 mg, 0.31 mmol) as a white solid after flash chromatography (*n*-hexane/ethyl acetate 6:1) on deactivated silica gel (2% Et_3N in *n*-hexane); yield 77%; m.p. 97–98 °C; $[\alpha]_D^{25} = -0.61°$ (c = 1.6 in $CHCl_3$); ^1H NMR (300 MHz, $CDCl_3$): δ = 0.74 (d, J = 6.9 Hz, 3H), 0.78 (d, J = 6.8 Hz, 3H), 1.39 (s, 9H), 1.43 (d, J = 6.9 Hz, 3H), 1.66 (br s, 1H), 1.75–1.81 (m, 1H), 2.77 (d, J = 5.5 Hz, 1H), 2.81–3.03 (m, 3H), 5.03–5.12 (m, 1H), 7.13–7.28 (m, 5H), 7.49 ppm (d, J = 7.5 Hz, 1H); ^{13}C NMR (75.5 MHz, $CDCl_3$): δ = 18.1(CH_3), 19.0 (CH_3), 21.5 (CH_3), 28.0 (CH_3), 31.4 (CH), 44.9 (C_q, ^3J(C,F) = 2.9 Hz), 48.9 (CH), 50.9 (C_q, ^2J(C,F) = 25.3 Hz), 68.0 (CH), 81.6 (CH), 124.6 (C_q, ^1J(C,F) = 280.6 Hz), 126.1 (CH), 127.2 (CH), 128.5 (CH), 142.9 (C), 164.7 (C_q, ^2J(C,F) = 2.3 Hz), 173.5 ppm (C); ^{19}F NMR (282.4 MHz, $CDCl_3$): δ =

© 2007 Wiley-VCH Verlag GmbH & Co. KGaA, Weinheim

−66.7 ppm (d, J (H,F) = 8.2 Hz, 3F); HRMS: m/z: calcd for $C_{21}H_{31}F_3N_2O_3$: 416.2286; found: 416.2272 $[M]^+$.

***tert*-Butyl (*S*)-3-methyl-2-[(*S*)-3,3,3-trifluoro-2-((*S*)-1-naphthalen-1-yl-ethylcarbamoyl)propylamino]butanoate (3gα)**: This compound was prepared by the general procedure described above, starting from **2g** (100 mg, 0.34 mmol) and (*S*)-**1d** (72 mg, 0.34 mmol), to afford **3gα** (133 mg, 0.29 mmol) as a white solid after flash chromatography (*n*-hexane/ethyl acetate 15:1) on deactivated silica gel (2% Et_3N in *n*-hexane); yield 84%; m.p. 110–111 °C; $[\alpha]_D^{25} = -14.2°$ (c = 0.9 in $CHCl_3$); ^{1}H NMR (300 MHz, $CDCl_3$): δ = 0.49 (d, J = 6.8 Hz, 3H), 0.56 (d, J = 6.8 Hz, 3H), 1.33 (br s, 1H), 1.35 (s, 9H), 1.50–1.56 (m, 1H), 1.63 (d, J = 6.8 Hz, 3H), 2.48 (d, J = 5.3 Hz, 1H), 2.72–3.00 (m, 3H), 5.83–5.93 (m, 1H), 7.33–7.49 (m, 4H), 7.58 (d, J = 7.7 Hz, 1H), 7.69–7.80 (m, 2H), 8.01 ppm (d, J = 8.3 Hz, 1H); ^{13}C NMR (75.5 MHz, $CDCl_3$): δ = 17.8 (CH_3), 18.7 (CH_3), 20.3 (CH_3), 28.0 (CH_3), 31.2 (CH), 44.7 (CH), 44.8 (C_q, ^3J(C,F) = 3.0 Hz), 50.8 (C_q, ^2J(C,F) = 24.3 Hz), 67.8 (CH), 81.4 (CH_3), 122.7 (CH), 123.2 (CH), 125.1 (CH), 125.7 (CH), 126.4 (CH), 127.4 (C_q, ^1J(C,F) = 278.4 Hz), 128.2 (CH), 128.7 (CH), 131.0 (C), 133.9 (C), 137.9 (C), 164.7 (C_q, ^3J(C,F) = 1.8 Hz), 173.5 ppm (C); ^{19}F NMR (282.4 MHz, $CDCl_3$): δ = −67.7 ppm (d, J (H,F) = 9.2 Hz, 3F); HRMS: m/z: calcd for $C_{25}H_{33}F_3N_2O_3$: 467.2521; found: 467.2476 $[M+H]^+$.

***tert*-Butyl (*S*)-3-methyl-2-{(*S*)-3,3,3-trifluoro-2-[((*S*)-1-naphthalen-1-yl-ethylamino)methyl]propionylamino}butanoate (3hα)**: This compound was prepared by the general procedure described above, starting from **2d** (100 mg, 0.33 mmol) and (*S*)-**1e** (57 mg, 54 μL, 0.33 mmol), to afford **3hα** (137 mg, 0.29 mmol) as a white solid after flash chromatography (*n*-hexane/ethyl acetate 6:1) on deactivated silica gel (2% Et_3N in *n*-hexane); yield 84%; m.p. 105–107 °C; $[\alpha]_D^{25} = +8.5°$ (c = 1.2 in $CHCl_3$); ^{1}H NMR (300 MHz, $CDCl_3$): δ = 0.82 (d, J = 6.8 Hz, 3H), 0.87 (d, J = 6.8 Hz, 3H), 1.42–1.44 (m, 12H), 1.50 (br, 1H), 2.07–2.17 (m, 1H), 2.81–2.88 (m, 1H), 2.97–3.00 (m, 1H), 3.01–3.15 (m, 1H), 4.42 (dd, J_1 = 8.7 Hz, J_2 = 4.5 Hz, 1H), 4.59 (q, J = 6.6 Hz, 1H), 6.96 (d, J = 8.3 Hz, 1H), 7.37–7.47 (m, 3H), 7.58 (d, J = 6.6 Hz, 1H), 7.69 (d, J = 8.1 Hz, 1H), 7.79–7.82 (m, 1H), 8.10 ppm (d, J = 8.7 Hz, 1H); ^{13}C NMR (75.5 MHz, $CDCl_3$): δ = 17.4 (CH_3), 18.8 (CH_3), 23.6 (CH), 31.1 (CH_3), 43.9 (C_q, ^3J(C,F) = 2.9 Hz), 51.3 (C_q, ^2J(C,F) = 25.3 Hz), 54.1 (CH), 57.8 (CH), 82.1 (C), 125.0 (C_q, ^1J(C,F)=280.5 Hz), 122.6 (CH), 122.7 (CH), 125.4 (CH), 125.6 (CH), 125.8 (CH), 127.4 (CH), 128.9 (CH), 131.1 (C), 133.9 (C), 140.2 (C), 165.6 (C_q, ^3J(C,F) = 2.3 Hz), 170.6 ppm (C); ^{19}F NMR (282.4 MHz, $CDCl_3$): δ = −70.4 ppm (d, J(C,F) = 9.2 Hz, 3F); HRMS: m/z: calcd for $C_{25}H_{33}F_3N_2O_3$: 466.2443; found: 466.2441 $[M]^+$.

(*S*)-2-[((*S*)-1-Cyclohexa-1,3-dienyl-ethylamino)methyl]-3,3,3-trifluoro-*N*-((*S*)-1-phenylethyl)propionamide (3kα): This compound was prepared by the general procedure described above, starting from **2e** (121 mg, 0.49 mmol) and (*S*)-**1f** (60 mg, 64 μL, 0.49 mmol), to afford **3kα** (105 mg, 0.29 mmol) as a white solid after flash chromatography (*n*-hexane/ethyl acetate 6:1) on deactivated silica gel (2% Et_3N in *n*-hexane); yield 60%; m.p. 122–124 °C; $[\alpha]_D^{25} = -38.9°$ (c = 0.9 in $CHCl_3$); ^{1}H NMR (300 MHz, $CDCl_3$): δ = 1.31 (d, J = 6.6 Hz, 3H), 1.50 (d, J = 6.8 Hz, 3H), 1.64 (br s, 1H), 2.71 (dd, J_1 = 12.5 Hz, J_2 = 3.4 Hz, 1H), 2.86–2.99 (m, 1H), 3.09–3.13 (m, 1H), 3.70 (q, J = 6.6 Hz, 1H), 5.11–5.19 (m, 1H), 7.21–7.40 (m, 10H), 7.76 ppm (d, J = 7.3 Hz, 1H); ^{13}C NMR (75.5 MHz, $CDCl_3$): δ = 21.5 (CH_3), 23.8 (CH_3), 43.7 (C_q, ^3J(C,F) = 2.9 Hz), 48.9 (CH), 50.7 (C_q, ^2J(C,F) = 24.7 Hz), 58.7 (CH), 124.7 (C_q, ^1J(C,F) = 280.5 Hz), 126.0 (CH), 126.5 (CH), 127.3 (CH), 127.4 (CH), 128.6 (CH), 128.6 (CH), 142.7 (C), 144.1 (C), 164.7 ppm (C_q, ^3J(C,F) = 2.3 Hz); ^{19}F NMR (282.4 MHz, $CDCl_3$) δ = −66.4 ppm (d, J(F,H) = 9.3 Hz, 3F); HRMS: m/z: calcd for $C_{20}H_{23}F_3N_2O$: 364.1762; found: 364.1784 $[M]^+$.

Computational methods: The potential energy surfaces corresponding to the reactions of the Michael acceptors **4a–c** (Figure 1) and (*S*)-**2l** and (*S*)-**2c** (Scheme 3) were explored by the density-functional method, at the B3LYP/6-31G* level of theory.[15] All the geometrical parameters were fully optimized, and the stationary points located were characterized as minima or saddle points, by performing the corresponding vibrational analysis. In addition, some stationary points were also located at the MP2/6-31G* level[15] (see Supporting Information for details). All the calculations were carried out with the Gaussian98 programs package.[29]

Acknowledgements

The authors thank the CIEMAT (MEC, Spain) for allocating computer time. A.M.R., G.Ch., and J.P. thank the regional government of the Principado de Asturias and the Ministerio de Educacion y Ciencia, respectively, for predoctoral fellowships. The authors thank the MEC (BQU2003-01610) and the Generalitat Valenciana (GR03-193) for financial support.

[1] Reviews: a) M. Misra, R. Luthra, K. L. Singh, K. Sushil, in *Comprehensive Natural Products Chemistry, Vol. 4* (Eds.: D. H. R. Barton, K. Nakanishi, O. Meth-Cohn), Pergamon, Oxford, UK, **1999**, p. 25; b) J. Staunton, B. Wilkinson, *Top. Curr. Chem.* **1998**, *195*, 49–92; see also: T. C. Wabnitz, J. B. Spencer, *Org. Lett.* **2003**, *5*, 2141–2144.

[2] a) M. Werder, H. Hausre, S. Abele, D. Seebach, *Helv. Chim. Acta* **1999**, *82*, 1774–1783; b) Y. Hamuro, J. P. Schneider, W. F. DeGrado, *J. Am. Chem. Soc.* **1999**, *121*, 12200–12201; c) K. Gademan, T. Kimmerlin, D. Hoyer, D. Seebach, *J. Med. Chem.* **2001**, *44*, 2460–2468; d) D. Liu, W. F. DeGrado, *J. Am. Chem. Soc.* **2001**, *123*, 7553–7559; e) J.-A. Ma, *Angew. Chem.* **2003**, *115*, 4426–4435; *Angew. Chem. Int. Ed.* **2003**, *42*, 4290–4299; f) N. Sewald, *Angew. Chem.* **2003**, *115*, 5972–5973; *Angew. Chem. Int. Ed.* **2003**, *42*, 5794–5795; g) J. Frackenpohl, P. I. Arvidsson, J. V. Schreiber, D. Seebach, *ChemBioChem* **2001**, *2*, 445–455; h) G. Lelais, D. Seebach, *Biopolymers* **2004**, *76*, 206–243; i) D. Seebach, D. F. Hook, A. Glättli, *Biopolymers* **2006**, *84*, 23–37.

[3] S. Kobayashi, K. Kakumoto, M. Sugiura, *Org. Lett.* **2002**, *4*, 1319–1322, and references therein.

[4] a) L.-W. Xu, Ch.-G. Xia, S.-L. Zhou, J.-W. Li, X.-X. Hu, *Synlett* **2003**, 2337–2340; b) review: M. Arend, B. Westermann, N. Risch, *Angew. Chem.* **1998**, *110*, 1096–1122; *Angew. Chem. Int. Ed.* **1998**, *37*, 1044–1070.

[5] a) *Enantioselective Synthesis of β-Amino Acid* (Eds.: E. C. Juaristi, V. A. Soloshonok), Wiley-VCH, Weinheim, 2nd ed., **2005**; b) J. Etxebarria, J. L. Vicario, D. Badia, L. Carrillo, N. Ruiz, *J. Org. Chem.* **2005**, *70*, 8790–8800 and references therein.

[6] For a recent review, see: L.-W. Xu, Ch.-G. Xia, *Eur. J. Org. Chem.* **2005**, 633–639.

[7] Only one example, to the best of our knowledge, involving a catalytic enantioselective conjugate addition of carbamates to β-alkyl-substituted α′-hydroxy enones has recently been described, by Palomo and co-workers. See, C. Palomo, M. Oiarbide, R. Halder, M. Kelso, E. Gómez-Bengoa, J. M. García, *J. Am. Chem. Soc.* **2004**, *126*, 9188–9189 and references therein.

[8] a) I. Ojima, *Chem. Rev.* **1988**, *88*, 1011–1030; b) T. Kitazume, T. Ohnogi, H. Miyauchi, T. Yamazaki, *J. Org. Chem.* **1989**, *54*, 5630–5632; c) Y. Hanzawa, M. Suzuki, Y. Kobayashi, T. Taguchi, Y. Iitaka, *J. Org. Chem.* **1991**, *56*, 1718–1725; d) T. Yamazaki, T. Ichige, S. Takei, S. Kawashita, T. Kitazume, T. Kubota, *Org. Lett.* **2001**, *3*, 2915–2918.

[9] I. Ojima, K. Kato, K. Nakahashi, T. Fuchikami, M. Fujita, *J. Org. Chem.* **1989**, *54*, 4511–4522.

[10] I. Ojima, F. A. Jameison, *Bioorg. Med. Chem. Lett.* **1991**, *1*, 581–584.

[11] a) D. Colantoni, S. Fioravanti, L. Pellacani, P. A. Tardella, *Org. Lett.* **2004**, *6*, 197–200; b) A. Avenoza, J. H. Busto, G. Jiménez-Osés, J. M. Peregrina, *J. Org. Chem.* **2005**, *70*, 5721–5724.

[12] Preliminary communication: M. Sani, L. Bruché, G. Chiva, S. Fustero, J. Piera, A. Volonterio, M. Zanda, *Angew. Chem.* **2003**, *115*, 2106–2109; *Angew. Chem. Int. Ed.* **2003**, *42*, 2060–2063.

[13] In the same way, Zanda, Volonterio, and co-workers previously designed a similar protocol for the synthesis of a new class of pseudopeptides starting, in this case, from β-trifluoromethyl acrylic acid derivatives and α-amino acid esters. a) A. Volonterio, P. Bravo, M. Zanda, *Org. Lett.* **2000**, *2*, 1827–1830; b) A. Volonterio, S. Bellosta, P. Bravo, E. Canavesi, E. Corradi, S. V. Meille, M. Monetti, N. Moussier, M. Zanda, *Eur. J. Org. Chem.* **2002**, 428–438; c) A. Volonterio, S. Bellosta, F. Bravin, M. C. Belluci, L. Bruché, G. Colom-

 © 2007 Wiley-VCH Verlag GmbH & Co. KGaA, Weinheim

bo, L. Malpezzi, S. Mazzini, S. V. Meille, M. Melli, C. R. de Arellano, M. Zanda, *Chem. Eur. J.* **2003**, *9*, 4510–4522; d) A. Volonterio, P. Bravo, M. Zanda, *Tetrahedron Lett.* **2001**, *42*, 3141–3144; e) M. Molteni, A. Volonterio, G. Fossati, P. Lazzari, M. Zanda, *Tetrahedron Lett.* **2007**, *48*, 589–592; f) M. Jagodzinska, F. Huguenot, M. Zanda, *Tetrahedron* **2007**, *63*, 2042–2046; g) M. Molteni, A. Volonterio, M. Zanda, *Org. Lett.* **2003**, *5*, 3887–3890.

[14] Other bases and solvents gave less satisfactory results (see ref. [12]).

[15] For a description of the theoretical methodology, see: F. Jensen, *Introduction to Computational Chemistry*, Wiley, Chichester, 2nd ed. **2007**.

[16] An analogous transition structure has previously been described in a study of the nucleophilic addition of ammonia to acrolein: L. Pardo, R. Osman, H. Weinstein, J. R. Rabinowitz, *J. Am. Chem. Soc.* **1993**, *115*, 8263–8269.

[17] M. Arnó, R. J. Zaragozá, L. R. Domingo, *Tetrahedron: Asymmetry* **2007**, *18*, 157–164.

[18] The authors would like to thank the referees for clarifying this point.

[19] For a detailed discussion of fluorine–hydrogen interactions see: K. Uneyama, *Organofluorine Chemistry*, Blackwell Publishing Ltd., Oxford **2006**, Chapter 4.

[20] For a classical presentation of Frontier Molecular Orbital theory, see: I. Fleming, *Frontier Orbitals and Organic Chemical Reactions*, Wiley, New York, **1982**.

[21] The LUMO energies (in eV) are as follows: **4a** (R = H, −0.762), **4b** (R = Me, −0.571), **4c** (R = F, −0.870), **4d** (R = CF_3, −1.360).

[22] Strictly speaking, the orbitals used in this work are Khon–Sham orbitals: that is, solutions of Khon–Sham density-functional equations (see ref. [15]), and not molecular orbitals in the most habitual sense of being solutions of the Hartree–Fock–Roothaan equations.

[23] A more detailed study of the concept of the electrophilicity, including a quantitative definition relating the energies of the HOMO and LUMO with a global electrophilicity index, can be found in: L. R. Domínguez, P. Pérez, R. Contreras, *Tetrahedron* **2004**, *60*, 6585–6591.

[24] a) C. E. Cannizzaro, T. Strassner, K. N. Houk, *J. Am. Chem. Soc.* **2001**, *123*, 2668–2669; b) C. E. Cannizzaro, K. N. Houk, *J. Am. Chem. Soc.* **2002**, *124*, 7163–7169.

[25] C. E. Cannizzaro, K. N. Houk, *J. Am. Chem. Soc.* **2004**, *126*, 10992–11008.

[26] D. Suárez, R. López, J. González, T. L. Sordo, J. A. Sordo, *Int. J. Quantum Chem.* **1996**, *57*, 493–499.

[27] A difference in energy of 0.8 kcal mol^{-1} at 0 °C produces a diastereoisomeric ratio (dr) of about 5:1.

[28] The full details of this experiment and the corresponding mathematical analysis can be found in the Supporting Information.

[29] Gaussian 98, Revision A.3, M. J. Frisch, G. W. Trucks, H. B. Schlegel, G. E. Scuseria, M. A. Robb, J. R. Cheeseman, V. G. Zakrzewski, J. A. Montgomery, Jr., R. E. Stratmann, J. C. Burant, S. Dapprich, J. M. Millam, A. D. Daniels, K. N. Kudin, M. C. Strain, O. Farkas, J. Tomasi, V. Barone, M. Cossi, R. Cammi, B. Mennucci, C. Pomelli, C. Adamo, S. Clifford, J. Ochterski, G. A. Petersson, P. Y. Ayala, Q. Cui, K. Morokuma, D. K. Malick, A. D. Rabuck, K. Raghavachari, J. B. Foresman, J. Cioslowski, J. V. Ortiz, B. B. Stefanov, G. Liu, A. Liashenko, P. Piskorz, I. Komaromi, R. Gomperts, R. L. Martin, D. J. Fox, T. Keith, M. A. Al-Laham, C. Y. Peng, A. Nanayakkara, C. Gonzalez, M. Challacombe, P. M. W. Gill, B. Johnson, W. Chen, M. W. Wong, J. L. Andres, C. Gonzalez, M. Head-Gordon, E. S. Replogle, J. A. Pople, Gaussian, Inc., Pittsburgh, PA, **1998**. http://www.gaussian.com

Received: March 9, 2007
Published online: July 20, 2007

 © 2007 Wiley-VCH Verlag GmbH & Co. KGaA, Weinheim